Materials Today Bio 17 (2022) 100470

Contents lists available at ScienceDirect

Materials Today Bio

journal homepage: www.journals.elsevier.com/materials-today-bio

The regulation role and diagnostic value of fibrinogen-like protein 1 revealed by pan-cancer analysis

Wanwan Yi [a,1], Tingting Qiao [a,1], Ziyu Yang [d,1], Lei Hu [c,1], Mingming Sun [c], Hengwei Fan [c,***], Yanping Xu [b,**], Zhongwei Lv [a,*]

[a] Department of Nuclear Medicine, Shanghai Tenth People's Hospital, Tongji University School of Medicine, Yanchang Middle Road 301, Shanghai, 200072, China
[b] School of Life Sciences and Technology, Tongji University, No.1239 SiPing Road, Yangpu District, Shanghai, 200092, China
[c] Department of Hepatic Surgery, The Eastern Hepatobiliary Surgery Hospital, Navy Medical University (Second Military Medical University), Shanghai, 200438, China
[d] Department of Integrated Chinese and Western Medicine, The Eastern Hepatobiliary Surgery Hospital, Navy Medical University (Second Military Medical University), Shanghai, 200438, China

ARTICLE INFO

Keywords:
Fibrinogen-like protein 1
Pan-cancer analysis
Immune infiltration
Genetic alteration
DNA methylation Status

ABSTRACT

Although the role of fibrinogen-like protein 1 (FGL1) in tumorigenesis is well known, a pan-cancer analysis of FGL1 lacks. We used bioinformatics techniques to analyze cancer data from publicly available datasets from The Cancer Genome Atlas, UALCAN, TIMER, Gene Expression Profiling Interactive Analysis, cBioPortal, Search Tool for the Retrieval of Interacting Genes, and DAVID. *FGL1* expression was significantly regulated in various common tumors than in normal tissues; it was increased in lung adenocarcinoma and decreased in colon adenocarcinoma. Cox regression analysis demonstrated that the upregulation of *FGL1* expression was correlated with poor overall survival (OS) and disease-free survival (DFS) in stomach adenocarcinoma, brain low-grade glioma, cervical squamous cell carcinoma, and endocervical adenocarcinoma. Decreased *FGL1* methylation levels were observed in majority of tumor types. *FGL1* expression was significantly associated with the levels of immune cell subtypes and immune checkpoint genes. Deep deletion was the most common genetic mutation in *FGL1* that led to frame-shift mutations, which was closely associated with poor progression-free interval, disease-specific survival, and OS in patients with *FGL1* mutations. Kyoto Encyclopedia of Genes and Genomes enrichment analysis showed that *FGL1*-related genes participate in diverse pathways. Ubiquitin-mediated proteolysis is significantly correlated to the function of FGL1, which was identified for the first time in the present study. This pan-cancer study provides a deep understanding of the functions of *FGL1* in progression of many tumors and demonstrates that *FGL1* may be a potential biomarker for the diagnosis, prognosis, and immune infiltration in cancer.

1. Introduction

Cancer has become a leading threat to global public health. In 2020, there were 19.3 million newly diagnosed cases and nearly 10 million cancer-related deaths [1], causing a significant economic burden on society. Currently, cancer treatment and prevention are crucial research directions [2]. Although great success has been achieved in the prevention, screening, diagnosis, and treatment of various tumors, the clinical outcomes of most cancers still need to be further studied [2,3]. A pan-cancer analysis can clarify the common characteristics and heterogeneity of human malignant tumors by analyzing the molecular abnormalities of various cancers [4]. This type of analysis is crucial for identifying new diagnostic, prognostic biomarkers and thereby novel and effective therapeutic targets. Therefore, pan-cancer analyses are considered highly important in cancer therapy and diagnosis, providing novel insights into the therapy and prevention of tumors [5–7].

The expression of fibrinogen-like protein 1 (FGL1)—an acute inflammatory factor secreted by the liver, also known as liver fibrinogen-related gene-1 (LFIRE-1)—is upregulated in various tumors, such as liver, pancreas, melanoma, lung, breast, colorectal, and prostate tumors. FGL1 is related to proliferation, metabolism, apoptosis, epithelial-to-

*** Corresponding author.
** Corresponding author.
* Corresponding author.
E-mail addresses: 1911608@tongji.edu.cn (W. Yi), Tting_qiao@163.com (T. Qiao), 569440303@qq.com (Z. Yang), leihu76@hotmail.com (L. Hu), sunminmin_ehbh@126.com (M. Sun), fanhengwei2006@163.com (H. Fan), yanpingxu@tongji.edu.cn (Y. Xu), Lvzwjs2020@163.com (Z. Lv).
[1] These authors contributed equally to the article.

https://doi.org/10.1016/j.mtbio.2022.100470
Received 29 July 2022; Received in revised form 7 October 2022; Accepted 18 October 2022
Available online 20 October 2022

Abbreviations

BLCA	Bladder urothelial carcinoma
BRCA	Breast invasive carcinoma
CESC	Cervical squamous cell carcinoma
CNA	Copy number alteration
COAD	Colon adenocarcinoma
CPTAC	Clinical Proteomic Tumor Analysis Consortium
DFS	Disease-free survival
DLBCL	Diffuse large B cell lymphoma
DSS	Disease-specific survival
ESCA	Esophageal carcinoma
GEPIA	Gene Expression Profiling Interactive Analysis
GSEA	Gene set enrichment analysis
HNSC	Head and neck squamous cell carcinoma
KEGG	Kyoto Encyclopedia of Genes and Genomes
KICH	Kidney chromophobe
KIRC	Kidney renal clear cell carcinoma
LGG	Low-grade glioma
LIHC	Liver hepatocellular carcinoma
LUAD	Lung adenocarcinoma
LUSC	Lung squamous cell carcinoma
OS	Overall survival
PRAD	Prostate adenocarcinoma
READ	Rectum adenocarcinoma
SKCM	Skin cutaneous melanoma
STAD	Stomach adenocarcinoma
STRING	Search Tool for the Retrieval of Interacting Genes
TCGA	The Cancer Genome Atlas
TGCT	Testicular germ cell tumor
THCA	Thyroid carcinoma
UCEC	Uterine corpus endometrial carcinoma
UCS	Uterine carcinosarcoma

mesenchymal transition, and immune infiltration [8,9]. FGL1 is a major immune inhibitory ligand of lymphocyte activation gene-3 (LAG-3) [10]. Both FGL1 and LAG3 are regarded as immune checkpoints in cancer [10], as the binding of FGL1 to LAG-3 can inhibit T cell activation and proliferation, forming an immunosuppressive pathway, different from that of PD-1/PD-L1 [9–11]. Specifically, FGL1 affects T cell function and cytokine production when LAG3 expression is upregulated [9], thereby playing an essential role in mediating tumor immunosuppression. Additionally, FGL1 is considered to be the next most important immune checkpoint target, which probably synergizes with PD-L1 to inhibit tumor immunity [9]. Recent studies have suggested that FGL1 is closely related with tumor progression and unfavorable prognosis in hepatocellular carcinoma [12–14], gastric cancer [15], clear cell renal cell carcinoma [16] and lung adenocarcinoma [17–19].

Given the heterogeneity of tumor types, a pan-cancer analysis is required to fully understand the possible role of *FGL1* in cancer progression and development—an aspect not extensively studied. The present study explored the regulation role and diagnostic value of *FGL1* in different tumors from various aspects, including gene expression, protein expression, methylation level, prognosis, genetic alteration, immune infiltration, and gene enrichment analysis, to determine the potential molecular mechanism of FGL1 in tumors.

2. Materials and methods

2.1. Gene expression analysis

Gene Expression Profiling Interactive Analysis (GEPIA; http://1gepia.cancer-pku.cn/) [20] was used to investigate the mRNA expression levels of FGL1 in tissues of 33 types of tumors and adjacent normal tissues in the Genotypic-Tissue Expression (GTEx) and The Cancer Genome Atlas (TCGA) databases. We used the UALCAN portal (http://ualcan.path.uab.edu) [21] to conduct a pan-cancer analysis of FGL1 using TCGA and the Clinical Proteomic Tumor Analysis Consortium (CPTAC). We also investigated the differences in FGL1 protein expression levels between tumor and normal tissues in various tumor datasets from CPTAC samples. Furthermore, we obtained boxplots of FGL1 expression in various cancer types at various pathological stages (including stages I, II, III, and IV) from TCGA.

Pan-cancer analyses of *FGL1* were conducted on the following 33 cancer types, data for which were retrieved from TCGA: adrenocortical carcinoma (ACC), bladder urothelial carcinoma (BLCA), breast invasive carcinoma (BRCA), cervical squamous cell carcinoma (CESC), cholangiocarcinoma (CHOL), colon adenocarcinoma (COAD), lymphoid neoplasm diffuse large B cell lymphoma (DLBCL), esophageal carcinoma (ESCA), glioblastoma (GBM), brain low-grade glioma (LGG), head and neck squamous cell carcinoma (HNSC), kidney chromophobe (KICH), kidney renal clear cell carcinoma (KIRC), kidney renal papillary cell carcinoma (KIRP), acute myeloid leukemia (LAML), liver hepatocellular carcinoma (LIHC), lung adenocarcinoma (LUAD), lung squamous cell carcinoma (LUSC), mesothelioma (MESO), ovarian serous cystadenocarcinoma (OV), pancreatic adenocarcinoma (PAAD), pheochromocytoma and paraganglioma (PCPG), prostate adenocarcinoma (PRAD), rectum adenocarcinoma (READ), sarcoma (SARC), skin cutaneous melanoma (SKCM), stomach adenocarcinoma (STAD), testicular germ cell tumor (TGCT), thyroid carcinoma (THCA), thymoma (THYM), uterine corpus endometrial carcinoma (UCEC), uterine carcinosarcoma (UCS), and uveal melanoma (UVM).

2.2. Survival analysis

Forest plots were used to explore the correlation between FGL1 expression and prognosis, including overall survival (OS) and disease-free survival (DFS), across cancers in TCGA dataset. Hazard ratios and 95% confidence intervals were calculated using a univariate survival analysis. The survival package (version 2.41–1) [22] in R was used to display the forest plots. $P < 0.05$ was considered a threshold.

In the GEPIA, we divided TCGA tumor samples into high- and low-expression groups according to the median expression of FGL1 in each cancer type. The OS and RFS of FGL1 in different cancers were analyzed and displayed using Kaplan-Meier curves.

2.3. Methylation analysis

To assess the association between FGL1 methylation level and cancers, we used the UALCAN website to obtain boxplots for FGL1 methylation levels in BLCA, BRCA, COAD, ESCA, HNSC, KIPR, LUSC, PRAD, READ, SARC, UCEC, and STAD from TCGA database.

2.4. Genetic alteration analysis

cBioPortal (https://www.cbioportal.org/) [23] is an online tool for investigating gene mutation frequency, mutation type, and copy number alterations (CNA). We used it to examine the genetic alterations of *FGL1* and conduct a mutation-related survival analysis in the pan-cancer cohort. We chose "TCGA Pan Cancer Atlas Studies" and entered "FGL1" in the "Quick select" selection for queries of the genetic alteration characteristics pan-cancer. We used the survival package in R 3.6.1 to visualize the association among OS, disease-specific survival (DSS), progression-free interval (PFI), DFI [24], and *FGL1* expression in all

patients, using a Kaplan-Meier gram.

2.5. Gene set enrichment analysis

First, the pan-cancer analysis results (including gene expression, protein expression, tumor-stage analysis, OS prognosis, DFS prognosis, and methylation status) were compared and visualized using the UpSetR 1.4.0 package [25] in R. Next, PAAD, LIHC, LGG, LUAD, LUSC, and THCA were selected for Kyoto Encyclopedia of Genes and Genomes (KEGG) analysis according to the significance associated with *FGL1* expression. We used Gene set enrichment analysis (GSEA; http://software.broadinstitute.org/gsea/index.jsp) to screen the KEGG signaling pathways associated with *FGL1* expression in PAAD, LIHC, LGG, LUAD, LUSC, and THCA. The criteria of significantly enriched pathways were normalized P < 0.05. The resulting enrichment pathways were visualized using the "ggplot2" package (version 3.3.5) in R-Studio.

2.6. Immune infiltration analysis

CIBERSORT (https://cibersort.stanford.edu/index.php) [26] and TIMER (http://timer.cistrome.org/) [27] algorithms were used to investigate the association between immune infiltrates and FGL1 expression across TCGA tumors. We then obtained heatmaps of Pearson's correlations between FGL1 expression and the abundance of different immune cell types. Subsequently, Pearson's method was used to determine the correlation between FGL1 expression and 23 common cancer immune checkpoint genes retrieved from the literature. The correlations were visualized in heatmaps using the "ggplot2" package (version 3.3.5) in R-Studio.

2.7. Protein–protein interaction network and enrichment analysis of FGL1

We used the Search Tool for the Retrieval of Interacting Genes (STRING; https://string-db.org/) [28] to construct the protein–protein interaction (PPI) network of *FGL1*-related genes. We considered an interaction with a combined score >0.150 as statistically significant. Visualization was performed using Cytoscape (version 3.6.1; http://www.cytoscape.org/) [29]—an open-source website platform for visualizing molecular interaction networks. We then conducted a KEGG analysis of *FGL1*-associated genes using DAVID (version 6.8, http://david.ncifcrf.gov) [30,31] to identify associated functions and pathways.

3. Results

3.1. Gene expression analysis

The mRNA expression of *FGL1* was inconsistent in 33 common human cancers, based on GEPIA results. The absolute expression of *FGL1* was the highest in LIHC, followed by CHOL, LUAD, and PAAD (Fig. 1A). Additionally, *FGL1* expression was significantly downregulated in tumors compared with that in adjacent normal tissues in the LGG, LIHC, PAAD, TGCT, and UCS datasets, whereas it was significantly upregulated in LUAD (Fig. 1B). We further compared the protein expression of FGL1 in the CPTAC database; FGL1 protein expression was significantly decreased in tumors compared with that in normal tissues in the OV, RCC, UCEC, HNSC, and PAA datasets, but was increased in the LIHC dataset (Fig. 1C).

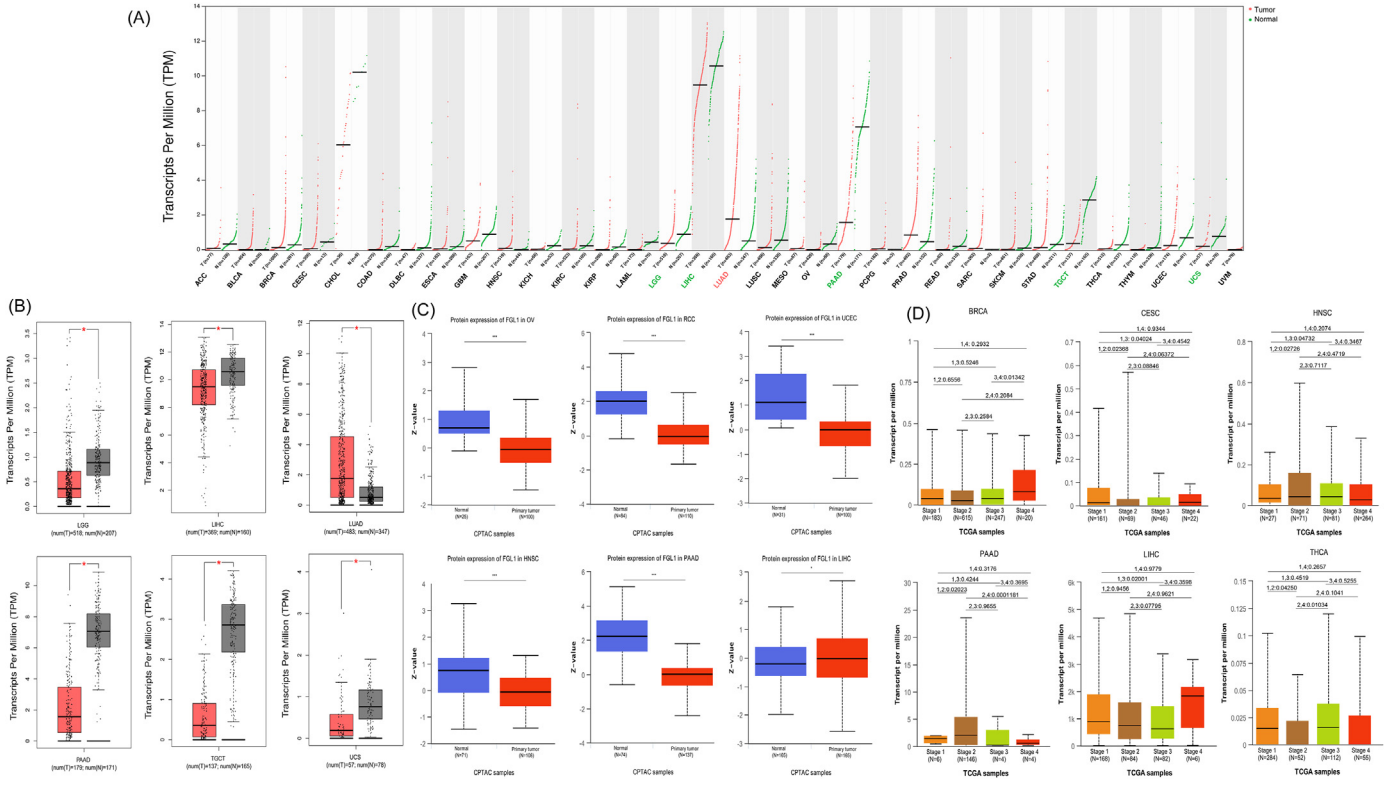

Fig. 1. Expression level of the *FGL1* gene in different tumors and pathological stages. (A) Expression levels of *FGL1* in different cancer types. The data were retrieved from TCGA in TIMER. The red and blue boxes represent tumor tissues and normal tissues, respectively. (B) For LGG, LIHC, LUAD, PAAD, TGCT, and UCS in TCGA, the corresponding normal tissues in the GTEx database are included as controls. The box plot data are provided. (C) FGL1 protein expression level in normal tissues and primary tissues of OV, RCC, UCEC, HNSC, PAAD, and LIHC examined using the CPTAC dataset. *P < 0.05, **P < 0.01, ***P < 0.001. (D) Relationship between FGL1 expression and main pathological stages, including stage I, stage II, stage III, and stage IV of BRCA, CESC, HNSC, PAAD, LIHC, and THCA examined based on TCGA data. The detailed P values were shown in Fig. 1D. (For interpretation of the references to color in this figure legend, the reader is referred to the Web version of this article.)

3.2. Correlation between FGL1 expression and clinicopathology

To study the relationship between FGL1 expression and clinicopathological features in various tumors, we assessed *FGL1* expression at different cancer stages (I–IV), using UALCAN. *FGL1* expression was significantly different at different tumor stages in BRCA, CESC, HNSC, PAAD, LIHC, and THCA, suggesting its role in cancer occurrence and development (Fig. 1D).

3.3. Survival analysis

We determined the prognostic effect of *FGL1* expression pan-cancer. First, the OS and DFS of FGL1 were analyzed by Cox regression analysis of the 33 tumor types in TCGA database. We constructed a forest plot of prognosis, which indicated that FGL1 expression was significantly related with OS in eight tumor types, namely, CESC, ESCA, KIRC, LGG, MESO, STAD, UCEC, and UCS (Fig. 2A). Upregulated FGL1 expression was a remarkable risk factor in patients with CESC, ESCA, KIRC, LGG, STAD, and UCS. In addition, FGL1 expression was significantly associated with the DFS for three tumor types: CESC, LGG, and STAD (Fig. 2B).

We performed OS analysis on the above data and obtained Kaplan-Meier survival curves (Fig. 2C). Results showed that the high expression of *FGL1* significantly associated with poor OS in CECS ($P = 0.023$), ESCA ($P = 0.025$), KIRC ($P = 0.013$), MESO ($P = 0.0079$), and UCS ($P = 0.023$). In contrast, low expression of *FGL1* significantly affected poor OS in STAD ($P = 0.02$), UCEC ($P = 0.0044$), and LGG ($P = 0.0078$). We also examined the association between *FGL1* expression and DFS of cancer patients (Fig. 2D). Kaplan-Meier analysis demonstrated that increased *FGL1* expression significantly influenced unfavorable DFS in CESC ($P = 0.0024$) and LGG ($P = 0.0017$). However, decreased *FGL1* expression was associated with poor DFS in STAD ($P = 0.0036$).

3.4. DNA methylation and genetic alterations

We examined the DNA methylation level of *FGL1* in different tumors using TCGA data on the UALCAN platform. The methylation level of *FGL1* was significantly decreased in BLCA, BRCA, COAD, ESCA, HNSC, KIPR, PRAD, READ, SARC, UCEC, and STAD tissues and increased in LUSC, compared with that in matched normal tissues (Fig. 3A).

Next, we examined the genetic alteration characteristics of *FGL1* in the pan-cancer cohort using the cBioPortal website (TCGA, Pan-Cancer Atlas). We used the "Cancer Types Summary" module to observe the mutation frequency, mutation type, and CNA of *FGL1* in all TCGA tumors. "Deep Deletion" was the most common type of genetic alteration, followed by "Mutation," "Amplification," "Structural Variant," and "Multiple Alterations" (Fig. 3B). The highest alteration frequency of *FGL1* was approximately 6.72% in LIHC, in which "Deep Deletion" was the most common genetic alteration type. Genetic alterations in FGL1 occurred more frequently in patients with COAD and BLCA.

We also investigated the potential association between genetic alterations in FGL1 and the prognosis of different types of tumors. Kaplan-Meier analysis (Fig. 3C) showed that patients with genetic alterations in FGL1 had unfavorable OS, Progression-free survival (PFS), and Disease specific survival (DSS) than patients without alterations. However, no significant difference was observed in DFS between the genetic alterations and control groups.

3.5. GSEA analysis

We performed GSEA and KEGG analyses to investigate the molecular mechanisms underlying *FGL1* regulation in diverse tumors. Briefly, GSEA was performed to examine the *FGL1*-associated signaling pathways that are differentially activated in cancer. We used gene expression, protein expression, stage, OS, DFS, and methylation status and screened the most significant tumors for KEGG analysis (PAAD, LIHC, LGG, LUAD, LUSC, and THCA; Fig. 4A). GSEA results of KEGG analysis revealed that 7, 11, 15, 23, 17, and 17 significantly *FGL1*-involved KEGG signaling pathways were obtained in PAAD, LIHC, LGG, LUAD, LUSC, and THCA, respectively (Fig. 4B and C). For example, in LGG, glycosaminoglycan biosynthesis keratan sulfate, complement and coagulation cascades, phenylalanine metabolism, pantothenate and CoA biosynthesis, O-glycan biosynthesis, cell adhesion molecules, starch and sucrose metabolism, retinol metabolism, leukocyte transendothelial migration, Fc gamma R-mediated phagocytosis, natural killer cell-mediated cytotoxicity, and PPAR signaling pathway were associated with *FGL1*. In LUAD, *FGL1* was found involved in various pathways, such as protein export, glyoxylate and dicarboxylate metabolism, aminoacyl-tRNA biosynthesis, riboflavin metabolism, ascorbate and aldarate metabolism, maturity-onset diabetes of the young, arginine and proline metabolism, nitrogen metabolism, porphyrin and chlorophyll metabolism, N-glycan biosynthesis, alanine aspartate and glutamate metabolism, pyruvate metabolism, cysteine and methionine metabolism, and adipocytokine signaling pathways. Furthermore, in LIHC, *FGL1* expression was correlated with several KEGG terms, such as complement and coagulation cascades, retinol metabolism, linoleic acid metabolism, ascorbate and aldarate metabolism, propanoate metabolism, steroid hormone biosynthesis, alanine aspartate and glutamate metabolism, arachidonic acid metabolism, and arginine and proline metabolism. The above results show that *FGL1*-associated signaling pathways are mainly involved in metabolic- and immune-associated pathways in these cancers, suggesting that *FGL1* plays an important role in cancer metabolism and immunity.

3.6. Analysis of immune cell infiltration and immune checkpoint genes

We used the TIMER database (including two methods: CIBERSORT and TIMER) to explore the relationship between *FGL1* expression and immune infiltration level in different tumors. *FGL1* expression was significantly associated with the abundance of infiltrating immune cells. Based on the TIMER algorithm analysis (Fig. 5A), we noted that *FGL1* had the highest positive correlation with neutrophils in ACC and the highest negative correlation with myeloid dendritic cells in DLBC. In addition, *FGL1* expression was negatively and significantly correlated with $CD8^+$ T cells, neutrophils, macrophages, and myeloid dendritic cells in LUAD patients. *FGL1* expression was positively correlated only with macrophages in LUSC. The expression of *FGL1* was positively correlated with neutrophils and myeloid dendritic cells in THCA, but negatively correlated with B cells.

We also used the CIBERSORT algorithm to investigate the association between FGL1 expression and infiltration of different immune cell subtypes. *FGL1* expression was significantly positively or negatively correlated with many immune cell subtypes in cancer (Fig. 5B). In LUAD, the expression of *FGL1* was positively correlated with B cell plasma, neutrophil, macrophage M0, Tregs, NK cell resting, and T cell follicular helper cells, while it was negatively correlated with macrophage M1, M2, monocyte, myeloid dendritic cell resting, and mast cell activated. In LUSC, $CD4^+$ T cell memory resting, $CD4^+$ T cell naïve, neutrophil, monocyte, and mast cell activated were positively associated with *FGL1* expression. In THCA, *FGL1* expression was positively associated with Tregs and myeloid dendritic cell resting, while negatively correlated with B cell plasma.

Furthermore, we examined the relationship between *FGL* expression and 23 genes of common immune checkpoints in a pan-cancer dataset. *FGL1* expression was correlated with 14 immune checkpoint genes in ACC, 13 in UVM, 20 in LUAD, 13 in THYM, and 17 in TGCT, and all P values were shown in Fig. 5C. The immune checkpoint gene *HAVCR2* was positively correlated with *FGL1* expression in ACC, and the immune checkpoint gene *IDO1* was negatively correlated with *FGL1* expression in UVM. These results suggest FGL1's significant role in tumor immunity.

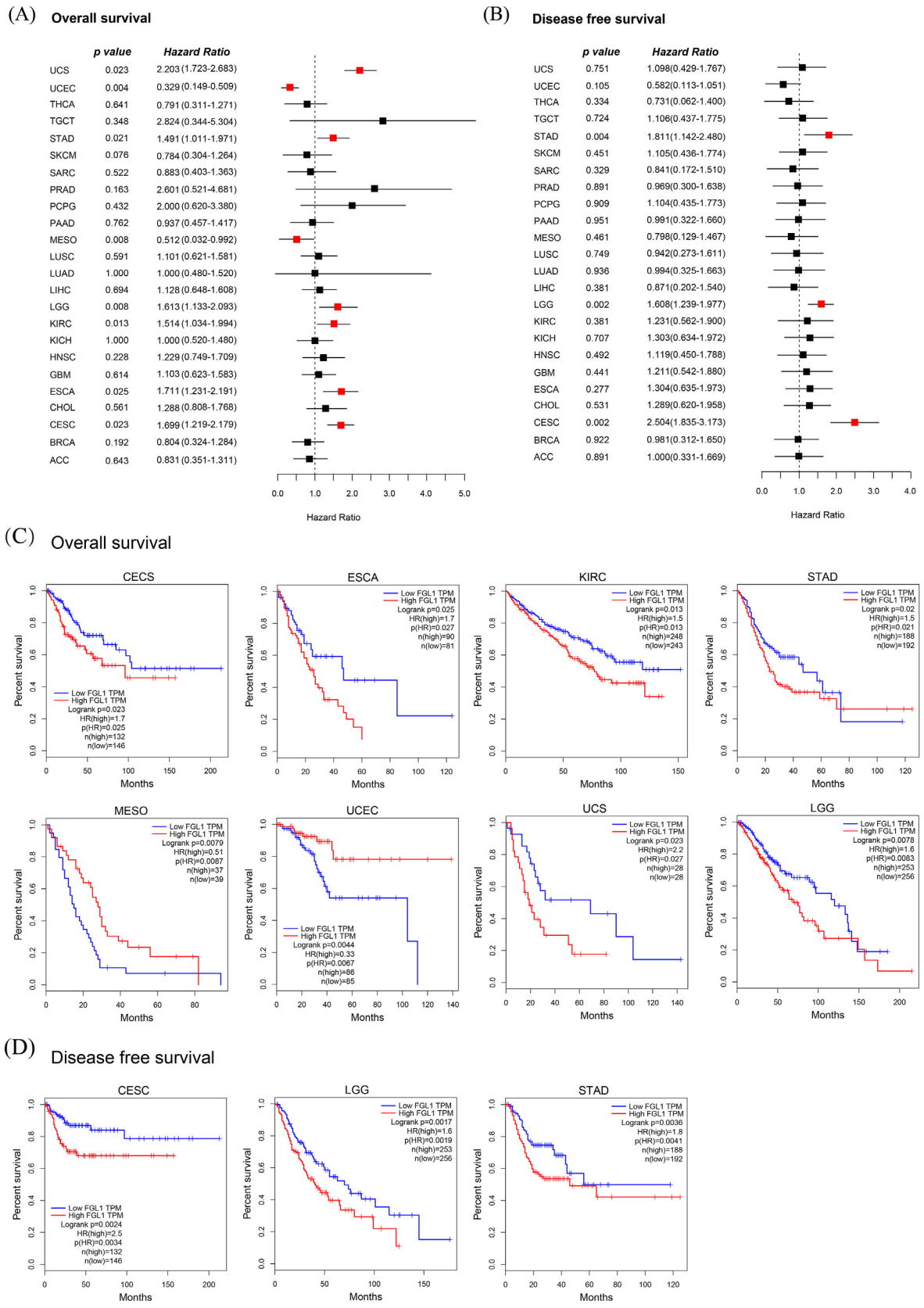

Fig. 2. Correlation between *FGL1* gene expression and survival prognosis of cancers in TCGA. Forest plot of (A) OS and (B) DFS in different cancers. The red squares indicate the tumor types that have a significant correlation with prognosis. (C) Kaplan-Meier survival curves of OS for patients stratified by the differential expression of *FGL1* in CESC, ESCA, KIRC, LGG, MESO, STAD, UCEC, and UCS. (D) Kaplan-Meier survival curves of DFS for patients stratified by the differential expression of *FGL1* in CESC, LGG, and STAD. The red and blue lines represent high and low expression, respectively. All P values were shown in Figure. (For interpretation of the references to color in this figure legend, the reader is referred to the Web version of this article.)

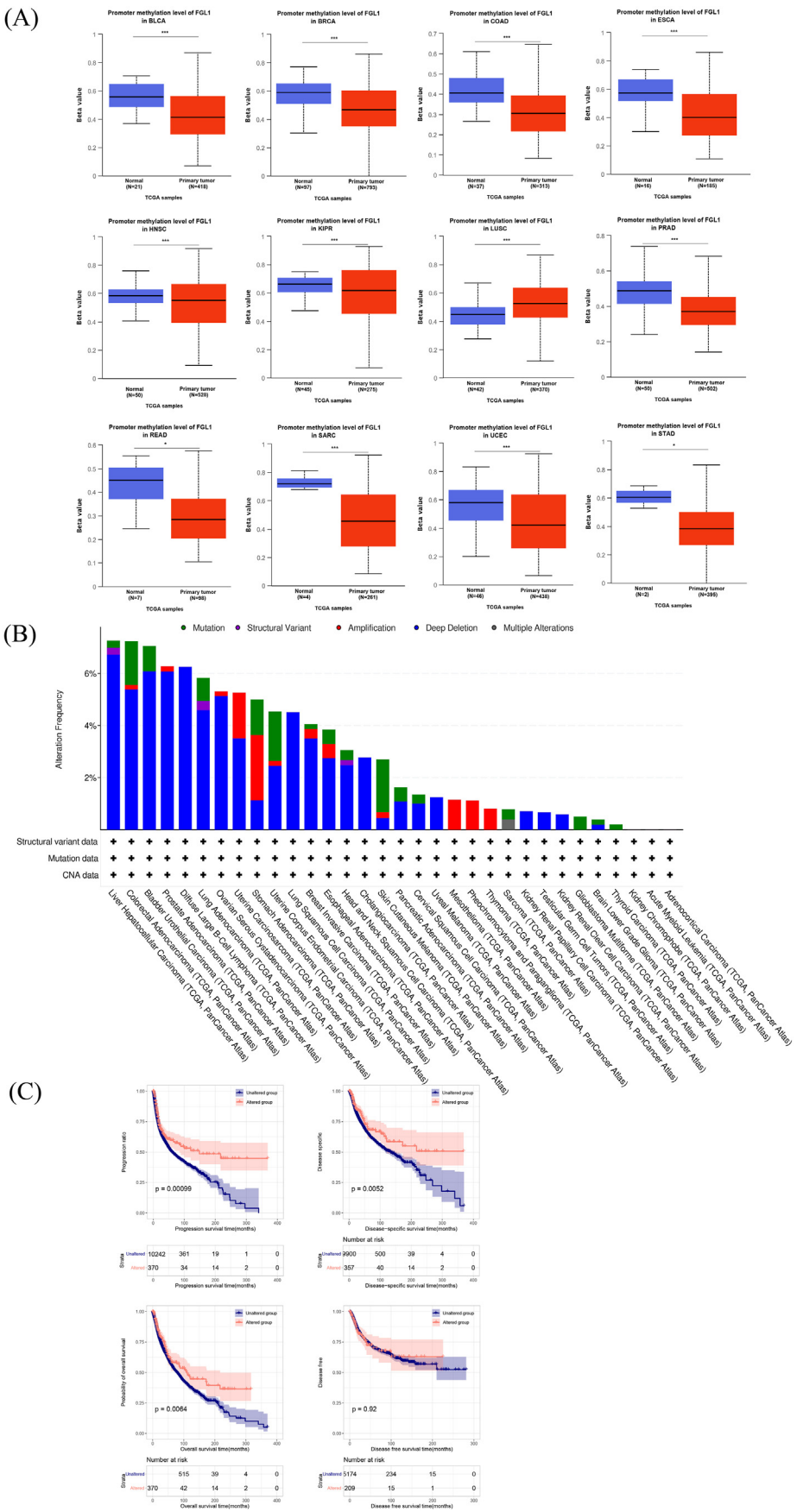

Fig. 3. DNA methylation and mutation feature of *FGL1* in different tumors of TCGA. (A) DNA methylation level of *FGL1* in BLCA, BRCA, COAD, ESCA, HNSC, KIPR, LUSC, PRAD, READ, SARC, UCEC, and STAD. The data were obtained from the UALCAN database. *P < 0.05, **P < 0.01, ***P < 0.001. (B) Alteration frequency with different mutations in *FGL1*. The results are displayed using the cBioPortal tool. (C) Effect of *FGL1* mutational status on overall, disease-specific, disease-free, and progression-free survivals of cancer patients assessed using the cBioPortal database. The detailed P values were shown in Fig. 3C.

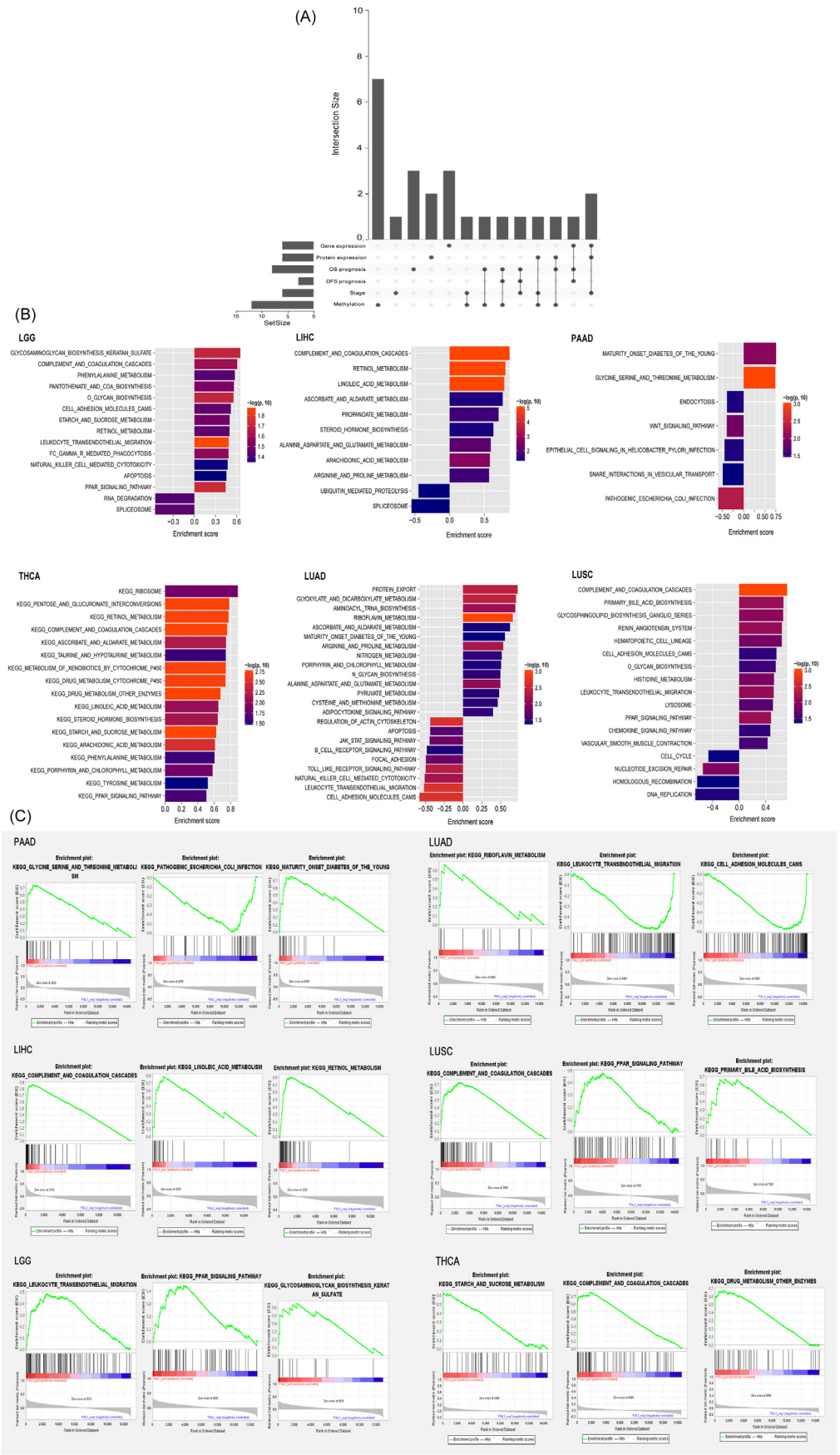

Fig. 4. Enrichment analysis for FGL1 obtained from KEGG. (A) Comparison of results with significance in different analysis of various tumors. (B) FGL1 signaling pathway analysis in PAAD, LIHC, LGG, LUAD, LUSC, and THCA. The horizontal axis represents the enrichment score, and the vertical axis represents the KEGG terms. The color of the column represents the significance; the closer to red, the higher the significance. (C) Top three KEGG pathways in which FGL1 is enriched in PAAD, LIHC, LGG, LUAD, LUSC, and THCA. (For interpretation of the references to color in this figure legend, the reader is referred to the Web version of this article.)

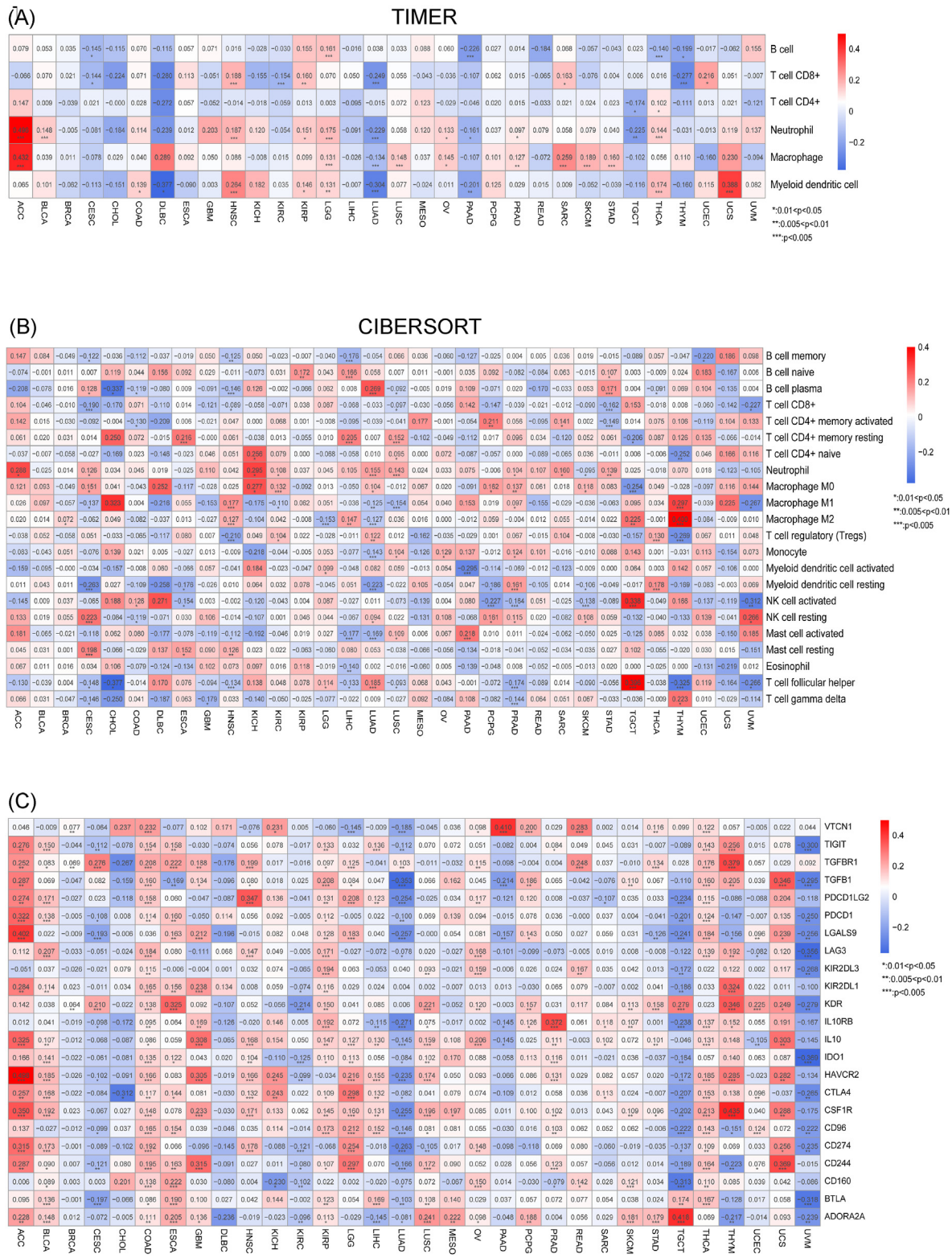

Fig. 5. Correlation of FGL1 expression with immune infiltration. (A) FGL1 expression is significantly correlated with the infiltration levels of various immune cells according to TIMER algorithm. *P < 0.05, **P < 0.01, ***P < 0.005. (B) FGL1 expression is significantly correlated with the infiltration levels of various immune cells based on the CIBERSORT algorithm. *P < 0.05, **P < 0.01, ***P < 0.005. (C) Correlation analysis of *FGL1* expression and 23 common immune checkpoint genes in different cancers. *P < 0.05, **P < 0.01, ***P < 0.005.

3.7. Functional enrichment analysis

Analyzing the functional interactions between proteins can provide a deeper understanding of the mechanisms of tumor formation and progression. We used the STRING tool to obtain 50 FGL1-related proteins and constructed a PPI network (Fig. 6A) and then conducted KEGG analysis for all related genes in the PPI network. The significant enriched pathways obtained in the KEGG pathway analysis (Table 1) were

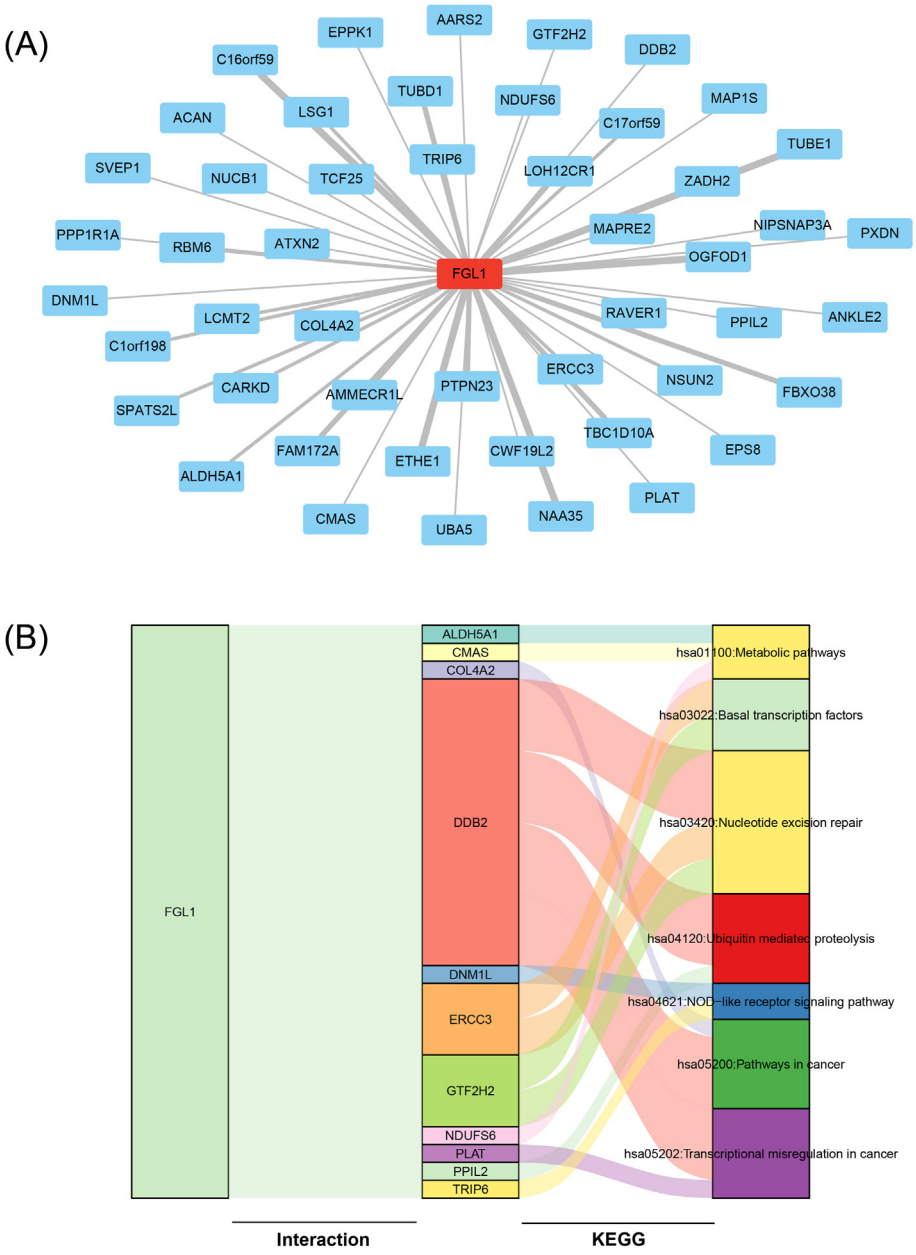

Fig. 6. Enrichment analysis of FGL1-related genes. (A) PPI network of top 50 genes related to the expression of FGL1. (B) Network diagram of the KEGG signaling pathways of the FGL1-interacting genes.

Table 1
KEGG classification terms of the FGL1-interacting genes.

Term	Count	Genes
hsa03420: Nucleotide excision repair	3	ERCC3, GTF2H2, DDB2
hsa03022: Basal transcription factors	2	ERCC3, GTF2H2
hsa04120: Ubiquitin mediated proteolysis	2	PPIL2, DDB2
hsa04621: NOD-like receptor signaling pathway	2	TRIP6, DNM1L
hsa05202: Transcriptional misregulation in cancer	2	PLAT, DDB2
hsa01100: Metabolic pathways	4	CMAS, ALDH5A1, NDUFS6, ETHE1
hsa05200: Pathways in cancer	2	COL4A2, DDB2

"nucleotide excision repair," "basal transcription factors," "ubiquitin-mediated proteolysis," "NOD-like receptor signaling pathway," "transcriptional misregulation in cancer," "metabolic pathways", and "pathways in cancer." Additionally, as shown in Fig. 6B, functional interaction network analysis demonstrated that *FGL1* interacted with eleven other genes and participated in seven functional pathways: For example, *FGL1* interacts with *ALDH5A1* and participates in "metabolic pathways"; interacts with *CMAS* and also participates in "metabolic pathways"; interacts with *COL4A2* and participates in "pathways in cancer"; interacts with *DDB2* and participates in "nuclear exercise repair," "ubiquitin-mediated proteolysis," "pathways in cancer" and "transcriptional misregulation in cancer"; interacts with *DMN1L* and participates in "NOD-like receiver signaling pathway"; interacts with *ERCC3/GTF2H2* and participates in "Basel transcription factors" and "nuclear accident repair"; interacts with *NDUFS6* and participates in "metabolic pathways"; interacts with plat to participate in "transcriptional misregulation in cancer"; interacts with *PPIL2* and participate in "ubiquitin-mediated proteolysis"; and interacts with *TRIP6* and participates in "NOD-like receiver signaling pathway."

4. Discussion

Cancer is a serious threat to human health owing to its high incidence and mortality rates [1]. Currently, the most common treatments for tumors are surgical resection, chemoradiotherapy, and immunotherapy; however, their efficacy remains limited [2]. Early prevention and effective treatment of cancer are critical for improving prognoses [3]. Pan-cancer analysis is an important bioinformatics approach that can provide novel and deeper insights into tumor prevention and personalized therapeutic strategies [5–7]. An increasing number of studies have strongly suggested that FGL1 is highly expressed in various tumor tissues and may serve as a pan-cancer prognostic biomarker [8,12,17]. Recent studies have shown that targeting FGL1 may serve as a new strategy for tumor immunotherapy [18,32–35]. However, the molecular mechanisms of FGL1 in different cancer types remain unclear and require further investigation. After a comprehensive literature search, we found no report on the pan-cancer analysis of FGL1. To our knowledge, this is the first study to comprehensively investigate *FGL1* expression in a pan-cancer dataset. We found that FGL1 plays important roles in the progression and prognosis of many tumors.

The results of pan-cancer analysis showed that *FGL1* was highly expressed in LUAD tissues as against their adjacent normal counterparts but the expression level decreased in LGG, LIHC, PAAD, TGCT, and UCS. Previous studies have shown that FGL1 not only promotes the invasion and metastasis of gastric [15] and liver cancer [13] but also inhibits tumor progression in *LKB1*-mutant LUAD [17], demonstrating that FGL1 has both pro-tumor and anti-tumor effects, which may due to the function and levels of different substrates. In addition, the overexpression of *FGL1* was related to worse prognosis (OS and DFS) in multiple tumors, such as CECS, ESCA, KIRC, and UCS, and the low expression of *FGL1* was correlated with poor OS in UCEC and MESO, suggesting that *FGL1* worked differently in different tumors. Notably, the expression of *FGL1* was closely related to immune infiltration and immune checkpoint markers in human cancers, especially ACC, UVM, and THYM, among others. Together, these results strongly indicate that FGL1 is a potential prognostic pan-cancer biomarker and plays a key role in tumor immunity.

Gene mutations can enhance the biological resistance of tumor cells to surrounding normal cells and are therefore a serious risk factor for tumorigenesis and progression [36]. Thus, genetic alteration of *FGL1* is likely to influence the expression levels of substrates. There are few studies on *FGL1* mutations in tumor tissues. In the present study, we used the cBioPortal tool to explore the mutation pattern and amplification frequency of *FGL1* in different tumors and found that the most common mutation of *FGL1* pan-cancer was deep deletion, manifesting as missense mutations at the protein level. Moreover, we investigated the potential relationship between genetic changes in *FGL1* and four prognosis outcomes and found that *FGL1* mutations had a significant impact on PFS, DSS, and OS of patients with malignant tumors. These findings suggest that genetic changes in *FGL1* play a significant role in tumorigenesis and unfavorable prognoses. We believe that both changes in *FGL1* expression levels alone and genetic alterations in *FGL1* affect tumor progression. DNA methylation is one of the earliest discovered and most well-studied epigenetic modifications in mammals, and it plays an important role in tumorigenesis and progression [37]. DNA methylation typically represses gene expression by altering chromatin structure, stability, and conformation [38]. Restoring key tumor suppressor genes through demethylation is essential for tumor prevention and treatment [39]. The findings of UALCAN illustrated that the methylation level of *FGL1* promoter was significantly decreased in multiple tumor tissues versus normal tissues, which may explain the altered regulation of *FGL1* expression in various cancers. Therefore, our study suggests a potential correlation between *FGL1* expression and DNA methylation. We did not retrieve the available literature on the methylation status of FGL1. However, the association between *FGL1* expression and DNA methylation levels requires further investigation.

The tumor microenvironment plays a dominant role in tumor initiation and progression, potentially accelerating tumor progression [40,41]. Although immunotherapy has made breakthroughs in tumor therapy [42–44], its clinical application and drug resistance (such as anti-PD-1/PD-L1 therapy) continue to face many challenges. Therefore, identifying new therapeutic targets and biomarkers is key to further improving the efficacy of immunotherapy and improving tumor resistance [45–47]. Recent studies have reported that the FGL1/LAG3 pathway is a promising immune checkpoint pathway [9–11], similar to PD-1/PD-L1, which plays an essential role in tumor immune escape mechanisms. Therefore, FGL1 is regarded as the next most important immune checkpoint and a promising novel therapeutic target for cancer [9]. Studies have demonstrated that FGL1 promotes cell proliferation in LUAD by regulating MYC target genes and can serve as an immune checkpoint [19]. In addition, it has been reported that FGL1 expression correlates with poor prognosis in HCC [13], plays an important role in immune microenvironment regulation, and results in PD-1/PD-L1 immunotherapy tolerance [9]. We observed that FGL1 expression was closely associated with multiple immune cells and immune checkpoint genes in various cancers, which is consistent with previous studies, strongly suggesting that FGL1 regulates or recruits immune cells to modulate tumor immunity and thus plays a complex role in tumor regulation. In present study, the analysis of immune cells and immune cell subsets based on TIMER and CIBERSORT shows a complex result, which needs further study. In addition, though TIMER and CIBERSORT are convenient and widely used methods to determine the level of immune infiltration, there are some inconsistent results between these two methods because of different algorithm. Therefore, further wet experiments, such as immunohistochemistry and flow cytometry are still warranted. Overall, the expression of *FGL1* is significantly related to various immune cells, which may indicate its role in immune regulation leading to the development of various tumors.

To further explore the role of FGL1 in tumors, we performed enrichment analysis of FGL1-related genes and proteins. FGL1-associated genes were found involved in "ubiquitin-mediated proteolysis" for the first time. Enrichment analyses also revealed that FGL1 is involved in some cancer-regulating processes, including "Nucleotide excision repair," "Basal transcription factors," "NOD-like receptor signaling pathway," "Transcriptional misregulation in cancer," "Metabolic pathways" and "Pathways in cancer," all of which are important in the occurrence and progression of cancer as well as in tumor cell proliferation. Our study is the first to show that *FGL1*, via its associated genes, probably plays an essential role in tumorigenesis by modulating ubiquitination. We also conducted KEGG analysis to investigate the function of *FGL1* in specific cancers, including PAAD, LIHC, LGG, LUAD, LUSC, and THCA, and found that *FGL1* participated in many signaling pathways, mainly associated with immune pathways and metabolic pathways.

Although we explored and analyzed the expression, survival prognosis, genetic alterations, DNA methylation status, immune infiltration, and KEGG enrichment analysis concerning FGL1, some limitations of this study should be acknowledged. First, we did not perform any wet-lab experiments on FGL1 expression in tumor tissues. Second, our study did not explore the cellular mechanisms of FGL1 in cancer. In the future, in vivo and in vitro experiments are required to validate our findings and further investigate the functional mechanisms of FGL1 expression in tumors.

5. Conclusions and perspectives

In conclusion, this pan-cancer study comprehensively and systematically explored the role of *FGL1* in tumors and demonstrated the effect of

FGL1 in progression of most cancer types. We speculate that *FGL1* promotes tumorigenesis and subsequent progression of diverse cancers via DNA methylation, genetic alterations, and the tumor microenvironment. The findings of this study support the position that *FGL1* is an important biomarker for the diagnosis, prognosis, and treatment target of several tumors. Our study provides insights into and directions for experimental studies on FGL1 expression in tumor immune research and therapeutic strategies targeting *FGL1*.

Author contributions

Wanwan Yi and Lei Hu: Data analysis and funding acquisition, Writing - original draft. **Tingting Qiao and Ziyu Yang:** Literature collection, Writing - original draft. **Hengwei Fan and Mingming Sun:** Funding acquisition and data analysis. **Yanping Xu:** Supervision, Funding acquisition, Writing - review & editing. **Zhongwei Lv:** Funding acquisition, Writing - review & editing.

Table S1
The roles of FGL1 in different cancers

Tumor type	Gene expression	Protein expression	Survival	DNA methylation	Genetic alteration	Immune infiltration
ACC	NS	NS	NS	NS	NS	Positive correlated with neutrophils (TIMER and CIBERSORT) and macrophage (TIMER)
BLCA	NS	NS	NS	Decreased	Deep deletion, mutation	Positive correlated with neutrophil (TIMER)
BRCA	NS	NS	NS	Decreased	Deep deletion, amplification, mutation	Positive correlated with macrophage M2 (CIBERSORT)
CESC	NS	NS	Overexpression of FGL1 was associated with poor OS and unfavorable DFS	NS	Deep deletion, mutation	Negative correlated with B cell and $CD8^+$ T cell (TIMER)Positive correlated with B cell plasma, neutrophil, Macrophage M0, NK cell resting, and Mast cell resting; negative correlated with B cell memory, $CD8^+$ T cell, Macrophage M1, myeloid dendritic cell resting, T cell follicular helper and T cell gamma delta (CIBERSORT)
CHOL	NS	NS	NS	NS	Deep deletion	Negative correlated with B cell plasma and T cell follicular helper (CIBERSORT)
COAD	NS	NS	NS	Decreased	Deep deletion, amplification, mutation	Positive correlated with myeloid dendritic cell (TIMER) Positive correlated with NK cell activated; negative correlated with B cell plasma, $CD4^+$ T cell memory activated and NK cell resting (CIBERSORT)
DLBC	NS	NS	NS	NS	Deep deletion	Negative correlated with myeloid dendritic cells (TIMER)
ESCA	NS	NS	High expression of FGL1 was associated with poor OS	Decreased	Deep deletion, amplification, mutation	Positive correlated with $CD4^+$ T cell memory resting, and mast cell resting; negative correlated with myeloid dendritic cell resting and NK cell activated (CIBERSORT)
GBM	NS	NS	NS	NS	Mutation	Negative correlated with T cell gamma delta (CIBERSORT)
HNSC	NS	Downregulation	NS	Decreased	Deep deletion, structural variant, mutation	Positive correlated with $CD8^+$ T cell, neutrophil and myeloid dendritic cell (TIMER) Positive correlated with macrophage M1, M2, and mast cell resting; negative correlated with B cell memory, B cell plasma, $CD8^+$ T cell, Tregs, mast cell activated and T cell follicular helper (CIBERSORT)
KICH	NS	NS	NS	NS	NS	Positive correlated with $CD4^+$ naïve T cell, neutrophil and macrophage M0
KIRC	NS	Downregulation	High expression of FGL1 was associated with poor OS	NS	Deep deletion	Negative correlated with $CD8^+$ T cell (TIMER) Positive correlated with neutrophil, macrophage M0, and Tregs; negative correlated with macrophage M1 and $CD8^+$ T cell (CIBERSORT)
KIRP	NS	NS	NS	Decreased	Deep deletion	Positive correlated with $CD8^+$ T cell, neutrophil and myeloid dendritic cell (TIMER) Positive correlated with B cell naïve (CIBERSORT)
LGG	Downregulation	NS	Low expression of FGL1 was associated with poor OS; increased FGL1 expression significantly influenced unfavorable DFS	NS	Deep deletion, mutation	Positive correlated with $CD8^+$ T cell, neutrophil and myeloid dendritic cell (TIMER) Positive correlated with myeloid dendritic cell activated, neutrophil, macrophage, and T cell follicular helper; negative correlated with macrophage M2 (CIBERSORT)
LIHC	Downregulation	Upregulation	NS	NS	Deep deletion, structural variant, mutation	Positive correlated with B cell naïve, $CD4^+$ T cell memory resting, and macrophage M2; negative correlated with B cell memory, mast cell activated, eosinophil and T cell follicular helper (CIBERSORT)

(*continued on next page*)

Table S1 (*continued*)

Tumor type	Gene expression	Protein expression	Survival	DNA methylation	Genetic alteration	Immune infiltration
LUAD	Upregulation	NS	NS	NS	Deep deletion, structural variant, mutation	Negative correlated with $CD8^+$ T cell, neutrophil, macrophage and myeloid dendritic cell (TIMER) Positive correlated with B cell plasma, neutrophil, macrophage M0, Tregs, NK cell resting, and T cell follicular helper; negative correlated with macrophage M1, M2, monocyte, myeloid dendritic cell resting, and mast cell activated (CIBERSORT)
LUSC	NS	NS	NS	Increased	Deep deletion	Positive correlated with macrophage (TIMER) Positive correlated with $CD4^+$ T cell memory resting, $CD4^+$ T cell naïve, neutrophil, monocyte, mast cell activated; negative correlated with B cell plasma, $CD8^+$ T cell, macrophage M1, and T cell follicular helper (CIBERSORT)
MESO	NS	NS	High expression of FGL1 was associated with poor OS	NS	Amplification	NS
OV	NS	Downregulation	NS	NS	Deep deletion, amplification	Positive correlated with neutrophil and macrophage (TIMER) Positive correlated with monocyte (CIBERSORT)
PAAD	Downregulation	Downregulation	NS	NS	Deep deletion, mutation	Negative correlated with B cell, neutrophil and myeloid dendritic cell (TIMER) Positive correlated with mast cell activated; negative correlated with myeloid dendritic cell activated (CIBERSORT)
PCPG	NS	NS	NS	NS	Amplification	Positive correlated with $CD4^+$ T cell memory activated, macrophage M0, and NK cell resting; negative correlated with myeloid dendritic cell resting, and NK cell activated (CIBERSORT)
PRAD	NS	NS	NS	Decreased	Deep deletion, amplification	Positive correlated with neutrophil and macrophage (TIMER) Positive correlated with neutrophil, macrophage M0, macrophage M1, monocyte, myeloid dendritic cell resting, and NK cell resting; negative correlated with NK cell activated, T cell follicular helper and T cell gamma delta (CIBERSORT)
READ	NS	NS	NS	Decreased		
SARC	NS	NS	NS	Decreased	Deep deletion, structural variant	Positive correlated with $CD8^+$ T cell and macrophage (TIMER) Positive correlated with $CD4^+$ T cell memory activated and neutrophil (CIBERSORT)
SKCM	NS	NS	NS	NS	Deep deletion, amplification, mutation	Positive correlated with macrophage (TIMER) Positive correlated with macrophage M0, and NK cell resting; negative correlated with neutrophil, myeloid dendritic cell resting, and NK cell activated (CIBERSORT)
STAD	NS	NS	Low expression of FGL1 was associated with poor OS and poor DFS	Decreased	Deep deletion, amplification, mutation	Positive correlated with macrophage (TIMER) Positive correlated with B cell naïve, and B cell plasma, neutrophil; negative correlated with $CD8^+$ T cell and $CD4^+$ T cell memory activated (CIBERSORT)
TGCT	Downregulation	NS	NS	NS	Deep deletion	Negative correlated with $CD4^+$ T cell and neutrophil (TIMER) Positive correlated with macrophage M2, NK cell activated, and T cell follicular helper; negative correlated with $CD4^+$ T cell memory resting, and macrophage M0 (CIBERSORT)
THCA	NS	NS	NS	NS	Mutation	Positive correlated with $CD4^+$ T cell, neutrophil, and myeloid dendritic cell; negative correlated with B cell (TIMER) Positive associated with Tregs and myeloid dendritic cell resting; negative correlated with B cell plasma (CIBERSORT)
THYM	NS	NS	NS	NS	Amplification	Negative correlated with B cell and $CD8^+$ T cell (TIMER) Positive correlated with macrophage M1, M2, and T cell gamma delta; negative correlated with $CD4^+$ T cell naïve, Tregs, and T cell follicular helper (CIBERSORT)
UCEC	NS	Downregulation	Low expression of FGL1 was associated with poor OS	Decreased	Deep deletion, amplification, mutation	Positive correlated with $CD8^+$ T cell (TIMER) Negative correlated with B cell memory (CIBERSORT)

(*continued on next page*)

Table S1 (*continued*)

Tumor type	Gene expression	Protein expression	Survival	DNA methylation	Genetic alteration	Immune infiltration
UCS	Downregulation	NS	High expression of FGL1 was associated with poor OS	NS	Deep deletion, amplification	Positive correlated with myeloid dendritic cell (TIMER) Positive correlated with NK cell resting; negative correlated with $CD8^+$ T cell, macrophage M1, NK cell activated and T cell follicular helper (CIBERSORT)
UVM	NS	NS	NS	NS	Deep deletion	

ACC, Adrenocortical carcinoma; BLCA, Bladder Urothelial Carcinoma; BRCA, Breast invasive carcinoma; CESC, Cervical squamous cell carcinoma and endocervical adenocarcinoma; CHOL, Cholangio carcinoma; COAD, Colon adenocarcinoma; DLBC, Lymphoid Neoplasm Diffuse Large B-cell Lymphoma; ESCA, Esophageal carcinoma; GBM, Glioblastoma multiforme; HNSC, Head and Neck squamous cell carcinoma; KICH, Kidney Chromophobe; KIRC, Kidney renal clear cell carcinoma; KIRP, Kidney renal papillary cell carcinoma; LGG, Brain Lower Grade Glioma; LIHC, Liver hepatocellular carcinoma; LUAD, Lung adenocarcinoma; LUSC, Lung squamous cell carcinoma; MESO, Mesothelioma; OV, Ovarian serous cystadenocarcinoma; PAAD, Pancreatic adenocarcinoma; PCPG, Pheochromocytoma and Paraganglioma; PRAD, Prostate adenocarcinoma; READ, Rectum adenocarcinoma; SARC, Sarcoma; SKCM, Skin Cutaneous Melanoma; STAD, Stomach adenocarcinoma; TGCT, Testicular Germ Cell Tumors; THCA, Thyroid carcinoma; THYM, Thymoma; UCEC, Uterine Corpus Endometrial Carcinoma; UCS, Uterine Carcinosarcoma; UVM, Uveal Melanoma; NS, not significant; OS, overall survival; DFS, disease-free survival.

Declaration of competing interest

The authors declare that they have no known competing financial interests or personal relationships that could have appeared to influence the work reported in this paper.

Data availability

Data will be made available on request.

Acknowledgement

We acknowledge the financial support from National Natural Science Foundation of China [grant number: 32000918, 82071964], Shanghai Tenth People's Hospital [grant number: 2021SYPDRC065], Shanghai Leading Talent Program sponsored by Shanghai Human Resources and Social Security Bureau [grant number: 2019], Shanghai Shenkang Three-year Action Project [grant number: SHDC2020CR2054B] and Shanghai Shenkang Hospital Development Center [grant number: 2022SKLY-09] and Shanghai Municipal Health Commission [grant number: 202040043, 20214Y0159].

References

[1] H. Sung, J. Ferlay, R.L. Siegel, M. Laversanne, I. Soerjomataram, A. Jemal, et al., Global cancer statistics 2020: globocan estimates of incidence and mortality worldwide for 36 cancers in 185 countries, CA A Cancer J. Clin. 71 (2021) 209–249, https://doi.org/10.3322/caac.21660.

[2] K.D. Miller, L. Nogueira, A.B. Mariotto, J.H. Rowland, K.R. Yabroff, C.M. Alfano, et al., Cancer treatment and survivorship statistics, CA A Cancer J. Clin. 69 (2019) 363–385, https://doi.org/10.3322/caac.21565, 2019.

[3] R.L. Siegel, K.D. Miller, A. Jemal, Cancer statistics, CA A Cancer J. Clin. 69 (2019) 7–34, https://doi.org/10.3322/caac.21551, 2019.

[4] J.N. Weinstein, E.A. Collisson, G.B. Mills, K.R. Shaw, B.A. Ozenberger, K. Ellrott, et al., The cancer genome atlas pan-cancer analysis project, Nat. Genet. 45 (2013) 1113–1120, https://doi.org/10.1038/ng.2764.

[5] Q. Ge, G. Li, J. Chen, J. Song, G. Cai, Y. He, et al., Immunological role and prognostic value of apbb1ip in pan-cancer analysis, J. Cancer 12 (2021) 595–610, https://doi.org/10.7150/jca.50785.

[6] C. Xu, Y. Zang, Y. Zhao, W. Cui, H. Zhang, Y. Zhu, et al., Comprehensive pan-cancer analysis confirmed that atg5 promoted the maintenance of tumor metabolism and the occurrence of tumor immune escape, Front. Oncol. 11 (2021), 652211, https://doi.org/10.3389/fonc.2021.652211.

[7] S. Wang, R. Wang, F. Gao, J. Huang, X. Zhao, D. Li, Pan-cancer analysis of the dna methylation patterns of long non-coding rna, Genomics 114 (2022), 110377, https://doi.org/10.1016/j.ygeno.2022.110377.

[8] J. Yu, J. Li, J. Shen, F. Du, X. Wu, M. Li, et al., The role of fibrinogen-like proteins in cancer, Int. J. Biol. Sci. 17 (2021) 1079–1087, https://doi.org/10.7150/ijbs.56748.

[9] W. Qian, M. Zhao, R. Wang, H. Li, Fibrinogen-like protein 1 (fgl1): the next immune checkpoint target, J. Hematol. Oncol. 14 (2021) 147, https://doi.org/10.1186/s13045-021-01161-8.

[10] A.P. Shi, X.Y. Tang, Y.L. Xiong, K.F. Zheng, Y.J. Liu, X.G. Shi, et al., Immune checkpoint lag3 and its ligand fgl1 in cancer, Front. Immunol. 12 (2021), 785091, https://doi.org/10.3389/fimmu.2021.785091.

[11] J. Wang, M.F. Sanmamed, I. Datar, T.T. Su, L. Ji, J. Sun, et al., Fibrinogen-like protein 1 is a major immune inhibitory ligand of lag-3, Cell 176 (2019) 334–347, https://doi.org/10.1016/j.cell.2018.11.010.

[12] M. Guo, F. Yuan, F. Qi, J. Sun, Q. Rao, Z. Zhao, et al., Expression and clinical significance of lag-3, fgl1, pd-l1 and cd8(+)t cells in hepatocellular carcinoma using multiplex quantitative analysis, J. Transl. Med. 18 (2020) 306, https://doi.org/10.1186/s12967-020-02469-8.

[13] Q. Yan, H.M. Lin, K. Zhu, Y. Cao, X.L. Xu, Z.Y. Zhou, et al., Immune checkpoint fgl1 expression of circulating tumor cells is associated with poor survival in curatively resected hepatocellular carcinoma, Front. Oncol. 12 (2022), 810269, https://doi.org/10.3389/fonc.2022.810269.

[14] H. Nayeb-Hashemi, A. Desai, V. Demchev, R.T. Bronson, J.L. Hornick, D.E. Cohen, et al., Targeted disruption of fibrinogen like protein-1 accelerates hepatocellular carcinoma development, Biochem. Biophys. Res. Commun. 465 (2015) 167–173, https://doi.org/10.1016/j.bbrc.2015.07.078.

[15] Y. Zhang, H.X. Qiao, Y.T. Zhou, L. Hong, J.H. Chen, Fibrinogenlikeprotein 1 promotes the invasion and metastasis of gastric cancer and is associated with poor prognosis, Mol. Med. Rep. 18 (2018) 1465–1472, https://doi.org/10.3892/mmr.2018.9097.

[16] Z. Lv, B. Cui, X. Huang, H.Y. Feng, T. Wang, H.F. Wang, et al., Fgl1 as a novel mediator and biomarker of malignant progression in clear cell renal cell carcinoma, Front. Oncol. 11 (2021), 756843, https://doi.org/10.3389/fonc.2021.756843.

[17] F. Bie, G. Wang, X. Qu, Y. Wang, C. Huang, Y. Wang, et al., Loss of fgl1 induces epithelialmesenchymal transition and angiogenesis in lkb1 mutant lung adenocarcinoma, Int. J. Oncol. 55 (2019) 697–707, https://doi.org/10.3892/ijo.2019.4838.

[18] C. Sun, W. Gao, J. Liu, H. Cheng, J. Hao, Fgl1 regulates acquired resistance to gefitinib by inhibiting apoptosis in non-small cell lung cancer, Respir. Res. 21 (2020) 210, https://doi.org/10.1186/s12931-020-01477-y.

[19] X.Y. Tang, Y.L. Xiong, A.P. Shi, Y. Sun, Q. Han, Y. Lv, et al., The downregulation of fibrinogen-like protein 1 inhibits the proliferation of lung adenocarcinoma via regulating myc-target genes, Transl. Lung Cancer Res. 11 (2022) 404–419, https://doi.org/10.21037/tlcr-22-151.

[20] Z. Tang, C. Li, B. Kang, G. Gao, C. Li, Z. Zhang, Gepia: a web server for cancer and normal gene expression profiling and interactive analyses, Nucleic Acids Res. 45 (2017) W98–W102, https://doi.org/10.1093/nar/gkx247.

[21] D.S. Chandrashekar, B. Bashel, S. Balasubramanya, C.J. Creighton, I. Ponce-Rodriguez, B. Chakravarthi, et al., Ualcan: a portal for facilitating tumor subgroup gene expression and survival analyses, Neoplasia 19 (2017) 649–658, https://doi.org/10.1016/j.neo.2017.05.002.

[22] P. Wang, Y. Wang, B. Hang, X. Zou, J.H. Mao, A novel gene expression-based prognostic scoring system to predict survival in gastric cancer, Oncotarget 7 (2016) 55343–55351, https://doi.org/10.18632/oncotarget.10533.

[23] J. Gao, B.A. Aksoy, U. Dogrusoz, G. Dresdner, B. Gross, S.O. Sumer, et al., Integrative analysis of complex cancer genomics and clinical profiles using the cbioportal, Sci. Signal. 6 (2013) l1, https://doi.org/10.1126/scisignal.2004088.

[24] H. Mizuno, K. Kitada, K. Nakai, A. Sarai, Prognoscan: a new database for meta-analysis of the prognostic value of genes, Bmc Med Genomics 2 (2009) 18, https://doi.org/10.1186/1755-8794-2-18.

[25] J.R. Conway, A. Lex, N. Gehlenborg, Upsetr: an r package for the visualization of intersecting sets and their properties, Bioinformatics 33 (2017) 2938–2940, https://doi.org/10.1093/bioinformatics/btx364.

[26] B. Chen, M.S. Khodadoust, C.L. Liu, A.M. Newman, A.A. Alizadeh, Profiling tumor infiltrating immune cells with cibersort, Methods Mol. Biol. 1711 (2018) 243–259, https://doi.org/10.1007/978-1-4939-7493-1_12.

[27] T. Li, J. Fu, Z. Zeng, D. Cohen, J. Li, Q. Chen, et al., Timer2.0 for analysis of tumor-infiltrating immune cells, Nucleic Acids Res. 48 (2020) W509–W514, https://doi.org/10.1093/nar/gkaa407.

[28] D. Szklarczyk, J.H. Morris, H. Cook, M. Kuhn, S. Wyder, M. Simonovic, et al., The string database in 2017: quality-controlled protein-protein association networks, made broadly accessible, Nucleic Acids Res. 45 (2017) D362–D368, https://doi.org/10.1093/nar/gkw937.

[29] P. Shannon, A. Markiel, O. Ozier, N.S. Baliga, J.T. Wang, D. Ramage, et al., Cytoscape: a software environment for integrated models of biomolecular interaction networks, Genome Res. 13 (2003) 2498–2504, https://doi.org/10.1101/gr.1239303.
[30] D.W. Huang, B.T. Sherman, R.A. Lempicki, Systematic and integrative analysis of large gene lists using david bioinformatics resources, Nat. Protoc. 4 (2009) 44–57, https://doi.org/10.1038/nprot.2008.211.
[31] D.W. Huang, B.T. Sherman, R.A. Lempicki, Bioinformatics enrichment tools: paths toward the comprehensive functional analysis of large gene lists, Nucleic Acids Res. 37 (2009) 1–13, https://doi.org/10.1093/nar/gkn923.
[32] W.J. Wan, G. Huang, Y. Wang, Y. Tang, H. Li, C.H. Jia, et al., Coadministration of irgd peptide with ros-sensitive nanoparticles co-delivering sifgl1 and sipd-l1 enhanced tumor immunotherapy, Acta Biomater. 136 (2021) 473–484, https://doi.org/10.1016/j.actbio.2021.09.040.
[33] C. Gong, X. Yu, W. Zhang, L. Han, R. Wang, Y. Wang, et al., Regulating the immunosuppressive tumor microenvironment to enhance breast cancer immunotherapy using ph-responsive hybrid membrane-coated nanoparticles, J. Nanobiotechnol. 19 (2021) 58, https://doi.org/10.1186/s12951-021-00805-8.
[34] S. Tabchi, N. Blais, Antiangiogenesis for advanced non-small-cell lung cancer in the era of immunotherapy and personalized medicine, Front. Oncol. 7 (2017) 52, https://doi.org/10.3389/fonc.2017.00052.
[35] D. Chai, D. Qiu, X. Shi, J. Ding, N. Jiang, Z. Zhang, et al., Dual-targeting vaccine of fgl1/caix exhibits potent anti-tumor activity by activating dc-mediated multi-functional cd8 t cell immunity, Mol Ther Oncolytics 24 (2022) 1–13, https://doi.org/10.1016/j.omto.2021.11.017.
[36] C.H. Yeang, F. Mccormick, A. Levine, Combinatorial patterns of somatic gene mutations in cancer, Faseb. J. 22 (2008) 2605–2622, https://doi.org/10.1096/fj.08-108985.
[37] H. Heyn, M. Esteller, Dna methylation profiling in the clinic: applications and challenges, Nat. Rev. Genet. 13 (2012) 679–692, https://doi.org/10.1038/nrg3270.
[38] M. Wang, V. Ngo, W. Wang, Deciphering the genetic code of dna methylation, Briefings Bioinf. 22 (2021), https://doi.org/10.1093/bib/bbaa424.
[39] Y.C. Liu, J. Kwon, E. Fabiani, Z. Xiao, Y.V. Liu, M.Y. Follo, et al., Demethylation and up-regulation of an oncogene after hypomethylating therapy, N. Engl. J. Med. 386 (2022) 1998–2010, https://doi.org/10.1056/NEJMoa2119771.
[40] B. Mlecnik, G. Bindea, F. Pages, J. Galon, Tumor immunosurveillance in human cancers, Cancer Metastasis Rev. 30 (2011) 5–12, https://doi.org/10.1007/s10555-011-9270-7.
[41] J. Galon, H.K. Angell, D. Bedognetti, F.M. Marincola, The continuum of cancer immunosurveillance: prognostic, predictive, and mechanistic signatures, Immunity 39 (2013) 11–26, https://doi.org/10.1016/j.immuni.2013.07.008.
[42] J.M. Zaretsky, A. Garcia-Diaz, D.S. Shin, H. Escuin-Ordinas, W. Hugo, S. Hu-Lieskovan, et al., Mutations associated with acquired resistance to pd-1 blockade in melanoma, N. Engl. J. Med. 375 (2016) 819–829, https://doi.org/10.1056/NEJMoa1604958.
[43] P.M. Forde, J.E. Chaft, K.N. Smith, V. Anagnostou, T.R. Cottrell, M.D. Hellmann, et al., Neoadjuvant pd-1 blockade in resectable lung cancer, N. Engl. J. Med. 378 (2018) 1976–1986, https://doi.org/10.1056/NEJMoa1716078.
[44] L. Kraehenbuehl, C.H. Weng, S. Eghbali, J.D. Wolchok, T. Merghoub, Enhancing immunotherapy in cancer by targeting emerging immunomodulatory pathways, Nat. Rev. Clin. Oncol. 19 (2022) 37–50, https://doi.org/10.1038/s41571-021-00552-7.
[45] F. Meric-Bernstam, J. Larkin, J. Tabernero, C. Bonini, Enhancing anti-tumour efficacy with immunotherapy combinations, Lancet 397 (2021) 1010–1022, https://doi.org/10.1016/S0140-6736(20)32598-8.
[46] S.M. Man, B.J. Jenkins, Context-dependent functions of pattern recognition receptors in cancer, Nat. Rev. Cancer (2022), https://doi.org/10.1038/s41568-022-00462-5.
[47] E.A. Rozeman, E.P. Hoefsmit, I. Reijers, R. Saw, J.M. Versluis, O. Krijgsman, et al., Survival and biomarker analyses from the opacin-neo and opacin neoadjuvant immunotherapy trials in stage iii melanoma, Nat. Med. 27 (2021) 256–263, https://doi.org/10.1038/s41591-020-01211-7.